Derivatives of (−)-7-Methyl-2-(5-(pyridinyl)pyridin-3-yl)-7-azabicyclo[2.2.1]heptane Are Potential Ligands for Positron Emission Tomography Imaging of Extrathalamic Nicotinic Acetylcholine Receptors

Yongjun Gao, Andrew G. Horti,* Hiroto Kuwabara, Hayden T. Ravert, John Hilton, Daniel P. Holt, Anil Kumar, Mohab Alexander, Christopher J. Endres, Dean F. Wong, and Robert F. Dannals

Division of Nuclear Medicine, Department of Radiology, The Johns Hopkins University School of Medicine, 600 North Wolfe Street, Baltimore, Maryland 21287-0816

Received February 26, 2007

A series of novel racemic 7-methyl-2-(5-(pyridinyl)pyridin-3-yl)-7-azabicyclo[2.2.1]heptane derivatives with picomolar in vitro binding affinity at nicotinic acetylcholine receptors (nAChRs) were synthesized and their enantiomers were resolved by semipreparative chiral HPLC. The (−)-enantiomers showed substantially greater in vitro inhibition binding affinity than the corresponding (+)-enantiomers. The compounds with best binding affinities have been radiolabeled with positron emitting isotopes ^{11}C and ^{18}F as potential radioligands for positron emission tomography imaging of the nAChR. In vivo enantioselectivity of the radiolabeled (−)-7-methyl-2-(5-(pyridinyl)pyridin-3-yl)-7-azabicyclo[2.2.1]heptane derivatives was observed in biodistribution studies in rodents and baboon. One of the radiolabeled compounds, (−)-7-methyl-2-*exo*-[3′-(2-[^{18}F]-fluoropyridin-5-yl))-5′-pyridinyl]-7-azabicyclo[2.2.1]heptane, exhibited good properties as a first practical PET radioligand for imaging of extrathalamic nAChR in baboon brain and holds promise for further investigation for human studies.

Introduction

Positron emission tomography (PET) is a key tool for noninvasive, in vivo studies of cerebral receptors, including nicotinic acetylcholine receptor (nAChR). PET has been widely used for studying neuronal nAChRs in neurodegenerative diseases and could be crucial for nAChR drug development. Research in this area started with initial attempts of PET imaging of nAChRs with ^{11}C-nicotine **1**,[1,2] a radioligand with low binding affinity. PET studies with the high affinity radiolabeled analogs of epibatidine, including **2** and **3** (Figure 1), yielded the first high-quality images of nAChRs in an animal brain (see for review, ref 3). The high toxicity of many radiolabeled epibatidine analogs, resulting from their properties as potent agonists of ganglionic $\alpha 3\beta 4$-nAChRs, has stimulated the search for less toxic radioligands based on radiolabeled analogs of A-85380 that have been recently used for quantitative PET imaging of nAChRs in human subjects. These analogs (**4** and **5**, Figure 1), while allowing the quantification of thalamic nAChR in human brain by PET, still present drawbacks that include slow brain kinetics and relatively low binding potentials.[3]

Development of PET radioligands for quantification of extrathalamic nAChR (ET[a] nAChR) is important due to a demonstration of altered densities of cortical and striatal nAChRs in neurodegenerative diseases.[4] Densities of nAChRs are lower in ET regions, and binding potential values in ET regions are lower than that in thalamus (Th). Therefore, radioligands with very high affinity are required for PET imaging of ET nAChR. Compounds [^{18}F]NIDA52189 **6** and [^{18}F]NIDA522131 **7** have been recently developed by us for imaging ET nAChR.[4] However, these radioligands exhibited prohibitively slow brain kinetics that require 8 h of PET scanning in the Rhesus monkey for the tracer radioactivity to reach a spatial-temporal steady state.[3] Such slow and almost irreversible brain kinetics is due to high hydrophilic properties of **6** and **7** ($\log D_{7.4} = \sim 0.5$ for both compounds **6** and **7**)[4] and their very high binding affinity ($K_i \sim 5$ pM for both compounds **6** and **7**).[4] The lipophilicity values of **6** and **7** is well below the optimal range of $\log D_{7.4} = 1-3$ for the high rate of blood−brain barrier (BBB) permeability.[5,6] An affinity that is too high may be prohibitive for the development of radioligands with sufficiently rapid brain kinetics.[7]

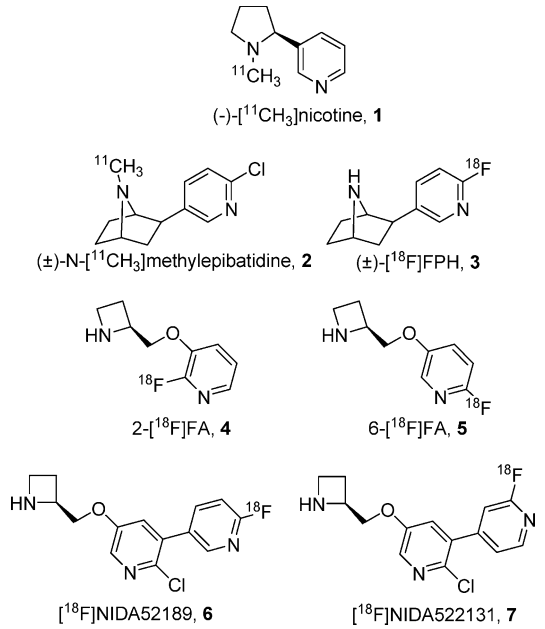

Figure 1. Representative PET radioligands for imaging nAChR.

Most recently there have been substantial efforts to design new PET nAChR radioligands with optimized binding affinity and lipophilicity and, thus, improved brain kinetics (**8**−**12**, Figure 2).[3,8−11] Some of these studies are based on 2-(5-substituted-pyridin-3-yl)-7-aza-bicyclo[2.2.1]heptane derivatives

* To whom correspondence should be addressed. Phone: 410-614-5130. Fax: 410-614-0111. E-mail address: ahorti1@jhmi.edu.

[a] Abbreviations: ET, extrathalamic; Th, thalamus; CB, cerebellum.

10.1021/jm070224t CCC: $37.00
Published on Web 07/13/2007

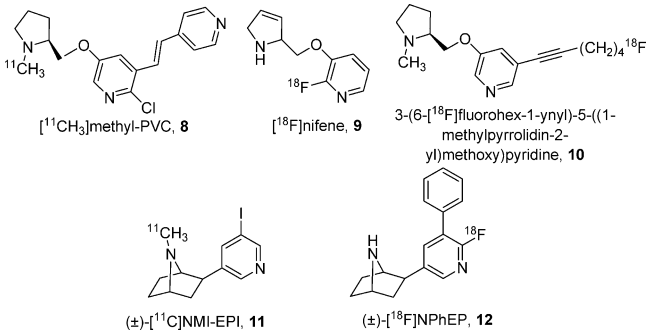

Figure 2. PET radioligands with rapid brain kinetics for imaging of thalamic nAChR.

Scheme 1. Synthesis of Compound (±)**17**[a]

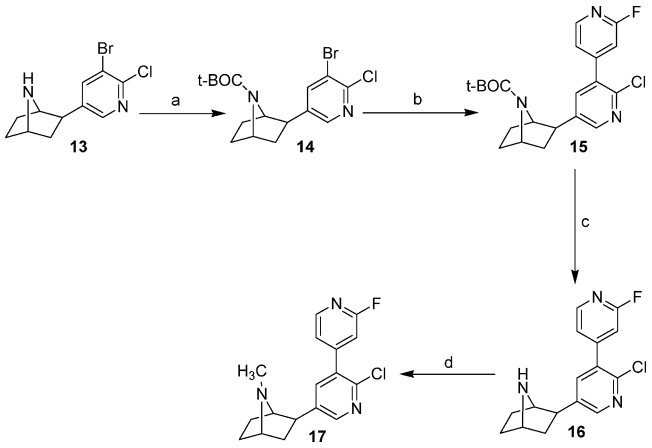

[a] Reagents: (a) $(Boc)_2O$, THF; (b) 2-fluoro-4-trimethyltinpyridine, $Pd(PPh_3)_4$/toluene; (c) CF_3COOH (TFA); (d) aqueous HCHO, $NaBH_3CN$.

that, in contrast to the toxic epibatidine analogs **2** and **3** (Figure 1), are nAChR antagonists or weak nAChR agonists that display low toxicity.[9,10,12,13] At least two such compounds, (±)-[^{11}C]-NMI-EPI **11** and (±)-[^{18}F]NPhEP **12** have been synthesized recently (Figure 2) and demonstrated promising properties (including "rapid" brain kinetics) for imaging thalamic nAChR in animals.[9,10]

The driving force of this research was a hypothesis that a radiolabeled 2-(5-substituted-pyridin-3-yl)-7-aza-bicyclo[2.2.1]-heptane derivative with a proper balance of binding affinity and lipophilicity can be suitable for PET imaging of ET nAChR while manifesting sufficiently rapid brain kinetics. Here we present development of (−)-7-methyl-2-*exo*-[3′-(2-[^{18}F]fluoro-pyridin-5-yl))-5′-pyridinyl]-7-azabicyclo[2.2.1]heptane [^{18}F]-(−)-**24d**, a radioligand with optimized values of in vitro binding affinity and lipophilicity for imaging of ET nAChR and a novel series of analogs of **24d**.

Results and Discussion

Chemistry. The 7-methyl-2-(5-(pyridinyl)pyridin-3-yl)-7-azabicyclo[2.2.1]heptane derivatives were prepared as shown in Schemes 1 and 2. Initial protection of amine **13**[14] with $(Boc)_2O$ provided compound **14** in good yield. The coupling of 3-bromopyridine derivative **14** with 2-fluoro-4-trimethyltin-pyridine via the Stille mechanism formed the corresponding bipyridine compound **15**. Secondary amine **16** was prepared by deprotection of **15** with trifluoroacetic acid (TFA). Compound **17** was obtained by reductive *N*-methylation of **16** with 37% formaldehyde in the presence of $NaBH_3CN$.

Suzuki coupling (Scheme 2) of 3-bromopyridines **18** and **19** with pyridylboronic compounds **20** and **21** gave bipyridine derivatives **22a**−**c**. Reaction of compound **22a** with sodium nitrite and copper(I) chloride produced the chlorinated derivative **23a**. Introduction of fluorine and removal of the protecting BOC group in compounds **23b** and **23c** were performed by fluorodediazoniation of **22a** and **22b**, correspondingly. Compound **23d** was prepared by deprotection of *N*-Boc derivative **22c**. *N*-Methyl derivatives **24a**−**d** were synthesized by reductive methylation of amines **23a**−**d** with formaldehyde in the presence of sodium phosphite.[15] The bromide derivative **26** was obtained by hydrolysis of the fluoride derivative **24d** and consecutive bromination of the intermediate pyridone **25**.

The racemic compounds **16**, **17**, **23c**, **23d**, **24c**, **24d**, and **26** were separated into their pure (+)- and (−)-enantiomers by semipreparative chiral HPLC (Chiralcel OD, Daicel, Inc.). The enantiomeric purity of each enantiomer was also determined by chiral HPLC (see Table 1).

N-Methylation of nor-methyl enantiomers **16**, **23c**, and **23d** with CH_3I in DMF stereoselectively gave *N*-methyl enantiomers **17**, **24c**, and **24d** with inversion of the sign of the specific optical rotation. Thus, methylation of (+)-**16**, (+)-**23c**, and (+)-**23d** stereoselectively yielded enantiomers (−)-**17**, (−)-**24c**, and (−)-**24d**, correspondingly; and the normethyl compounds (−)-**16**, (−)-**23c**, and (−)-**23d** produced the corresponding (+)-*N*-methyl enantiomers (+)-**17**, (+)-**24c**, and (+)-**24d**. Remarkably, methylation of enantiomers of nornicotine produces nicotine enantiomers with the same sign of optical rotation.[1] Swiss researchers demonstrated that methylation of enantiomers of epibatidine stereoselectively gives *N*-methylepibatidine enantiomers with the same sign of optical rotation: (−)-epibatidine yields (−)-*N*-methylepibatidine and vice versa, (+)-epibatidine yields (+)-*N*-methylepibatidine.[16] The reason for the inversion of the sign of the optical rotation coefficient of 7-methyl-2-(5-(pyridinyl)pyridin-3-yl)-7-azabicyclo[2.2.1]heptane analogs **17**, **24c**, and **24d** is currently unclear, but it is unlikely to involve an inversion of the absolute configuration of the molecules.

Structure−Activity Relationships. The series of racemic 2-(5-(pyridinyl)pyridin-3-yl)-7-azabicyclo[2.2.1]heptane derivatives **16**, **17**, **23d**, and **24a**−**d** were prepared in the course of this study. These ligands exhibited inhibition binding affinity values (K_i) in the range of 16−112 pM versus 45 ± 9 pM for the reference compound epibatidine **2** (Table 2), and their experimentally determined lipophilicities were in the range of $\log D_{7.4} = 0.2-1.4$. In contrast with 2-(5-(phenyl)pyridin-3-yl)-7-azabicyclo[2.2.1]heptane derivatives,[12] the affinity of 2-(5-(pyridinyl)pyridin-3-yl)-7-azabicyclo[2.2.1]heptane derivatives is tolerant to the presence and nature of a substituent in the position 2 of the internal pyridine ring. Thus, binding affinities of compounds (±)-**24a** (2-Cl), (±)-**24b** (2-F), and **24d** (2-H) are nearly the same. This finding permitted us to obtain a subseries of structurally similar analogs **24a**, **24b**, and **24d** with almost equal binding affinity but with various lipophilicities (Table 2).

Previous studies demonstrated that epibatidine analogs having a secondary aliphatic nitrogen atom display little enantioselectivity in the in vitro binding assay.[17] In contrast, nor-methyl compound (−)-**23d** displayed 2-fold binding affinity relatively (+)-**23d**.

Previously, Daly's group showed a relatively small enantioselectivity of (−)-*N*-methylepibatidine ($K_i = 0.11$ nM) versus (+)-*N*-methylepibatidine ($K_i = 0.26$ nM).[17] Nevertheless, the ^{11}C-radiolabeled enantiomers of *N*-methylepibatidine exhibited fairly different imaging properties in vivo.[18] The *N*-methyl enantiomers (−)-**17**, (−)-**24c**, and (−)-**24d** manifest conspicuous enantioselectivity of in vitro binding affinities in comparison

Scheme 2[a]

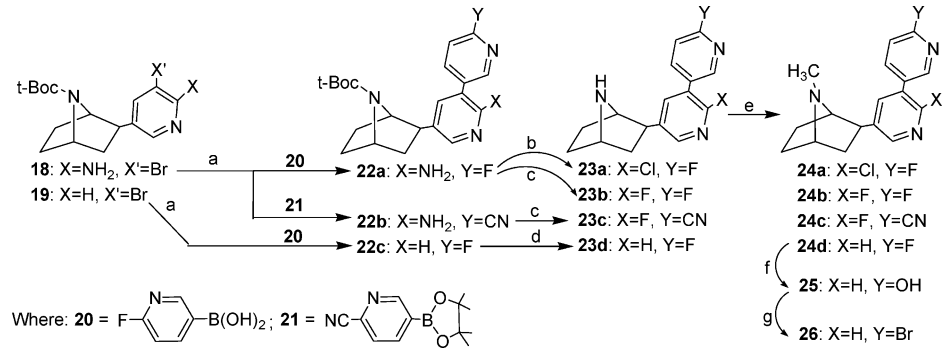

[a] Reagents: (a) $Pd(OAc)_2$, P(*o*-tolyl)$_3$, Na_2CO_3, DME; (b) HCl, CuCl, $NaNO_2$; (c) $NaNO_2$, HF-pyridine; (d) CF_3COOH (TFA); (e) NaH_2PO_3, 37% HCHO; (f) HCOOH; (g) PBr_3.

Table 1. Enantiomers of **16**, **17**, **23c**,**d** and **24c**,**d** Purified by Semipreparative Chiral HPLC (Chiralcel OD)

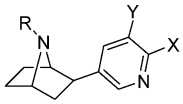

16 R=H, X=Cl, Y=2-fluoropyridin-4-yl
17 R=CH_3, X=Cl, Y=2-fluoropyridin-4-yl
23c R=H, X=F, Y=6-cyanopyridin-3-yl
24c R=CH_3, X=F, Y=6-cyanopyridin-3-yl
23d R=H, X=H, Y=6-fluoropyridin-3-yl
24d R=CH_3, X=H, Y=6-fluoropyridin-3-yl
26 R=CH_3, X=H, Y=6-bromopyridin-3-yl

enantiomer	chiral HPLC eluent (hexane/*i*-PrOH/Et_3N)	retention time (t_R, min)	ee[a] (%)	$[\alpha]^{22}_D$ ($CHCl_3$)	physical properties
(−)-**16**	100:400:2	11.5	>98	−0.14 (c = 0.75)	colorless oil
(+)-**16**	100:400:2	13.9	>98	+2.36 (c = 0.81)	colorless oil
(−)-**17**	20:480:1.5	11.5	>98	−18.99 (c = 0.78)	colorless oil
(+)-**17**	20:480:1.5	12.7	>98	+17.96 (c = 0.81)	colorless oil
(−)-**23c**	200:300:2	15.2	>98	−3.01 (c = 0.47)	yellow solid mp 99−100 °C
(+)-**23c**	200:300:2	10.96	>98	+3.62 (c = 0.57)	yellow solid mp 103−104 °C
(−)-**24c**	70:430:2	12.4	>98	−23.27 (c = 0.43)	white solid mp 140−141 °C
(+)-**24c**	70:430:2	14.1	>98	19.37 (c = 0.45)	white solid mp 139−140 °C
(−)-**23d**	100:400:2	13.9	>98	−8.38 (c = 1.00)	colorless oil
(+)-**23d**	100:400:2	15.1	>98	+8.31 (c = 1.00)	colorless oil
(−)-**24d**	50:450:2	9.6	>98	−18.94 (c = 0.84)	colorless oil
(+)-**24d**	50:450:2	10.8	>98	19.35 (c = 0.77)	colorless oil
(−)-**26**	50:450:2	12.0	>98	−19.7 (c = 0.83)	white solid mp 142−143 °C
(+)-**26**	50:450:2	13.4	>98	19.6 (c = 0.77)	white solid mp 143−144 °C

[a] ee = enantiomeric excess.

with corresponding enantiomers (+)-**17**, (+)-**24c**, and (+)-**24d** (Table 2). The pronounced enantioselectivity of the 7-methyl-2-(5-(pyridinyl)pyridin-3-yl)-7-azabicyclo[2.2.1]heptanes **17**, **24c**, and **24d** presented here is similar to that of nicotine (i.e., exhibiting a 38-fold enantioselectivity of binding affinity of (−)-nicotine versus (+)-nicotine).[17]

Radiochemistry. All of the ligands in the series demonstrated high binding affinity for nAChRs along with an optimal range of lipophilicity[3,5] for PET radiotracers (Table 2). Both the high binding affinity and the lipophilicity data suggest that these ligands are potential candidates for radiolabeling and PET studies. We radiolabeled (±)-**17** and (−)-**17**, the compounds with highest binding affinity within the series, with [^{11}C] (Scheme 3) and performed evaluation of radioligands [^{11}C]-(±)-**17** and [^{11}C]-(−)-**17** with small animal PET to assess their potential to image nAChRs in vivo.

The radiosynthesis of [^{11}C]-(±)-**17** (because racemic (±)-**17** was prepared initially in this study) and [^{11}C]-(−)-**17** was performed by reaction of corresponding nor-methyl derivatives

Table 2. Experimental Inhibition Binding Affinity (K_i) and Lipophilicity ($logD_{7.4}$) of Novel nAChR Ligands **16**, **17**, **23d**, and **24a**−**d** and a High Affinity Reference Ligand (±)-Epibatidine (2)

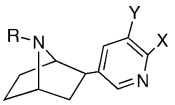

ligand	R	X	Y	K_i,[a] pM	$logD_{7.4}$[b]
epibatidine (**2**)	H	Cl	H	45 ± 9 (n = 15)	-
(±)-**16**	H	Cl	2-fluoropyridin-4-yl	14	0.77
(±)-**17**	CH_3	Cl	2-fluoropyridin-4-yl	53	1.26
(+)-**17**	CH_3	Cl	2-fluoropyridin-4-yl	309/207	
(−)-**17**	CH_3	Cl	2-fluoropyridin-4-yl	16/17	
(±)-**23a**	H	Cl	6-fluoropyridin-3-yl	52	0.68
(±)-**23d**	H	H	6-fluoropyridin-3-yl	112	0.16
(+)-**23d**	H	H	6-fluoropyridin-3-yl	223	
				183	
(−)-**23d**	H	H	6-fluoropyridin-3-yl	109	
				12	
				9	
(±)-**24a**	CH_3	Cl	6-fluoropyridin-3-yl	70	1.42
(±)-**24b**	CH_3	F	6-fluoropyridin-3-yl	73	0.96
				78	
(±)-**24c**	CH_3	F	6-cyanopyridin-3-yl	30	0.64
				60	
(+)-**24c**	CH_3	F	6-cyanopyridin-3-yl	797	
				955	
(−)-**24c**	CH_3	F	6-cyanopyridin-3-yl	18	
				21	
(±)-**24d**	CH_3	H	6-fluoropyridin-3-yl	74	0.45
(+)-**24d**	CH_3	H	6-fluoropyridin-3-yl	2170	
				2080	
(−)-**24d**	CH_3	H	6-fluoropyridin-3-yl	52	
				51	

[a] The in vitro inhibition binding assays of all compounds were performed commercially by NovaScreen Biosciences, a Caliper Life Science Co. (Hanover, MD), under conditions similar to those previously published,[26] using rat cortical membranes as a source of nAChRs and [^{3}H]epibatidine as a radioprobe. [b] The partition coefficient between *n*-octanol and sodium phosphate buffer at pH 7.4 ($logD_{7.4}$) was determined by a conventional shake-flask method in quadruplicate. These lipophilicity values correspond to an optimal range for the most known PET radiotracers.[5]

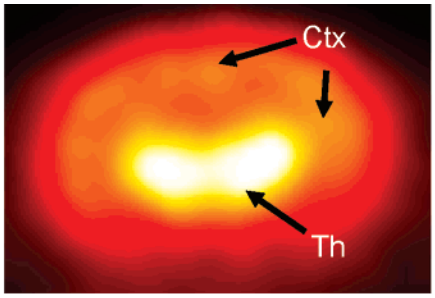

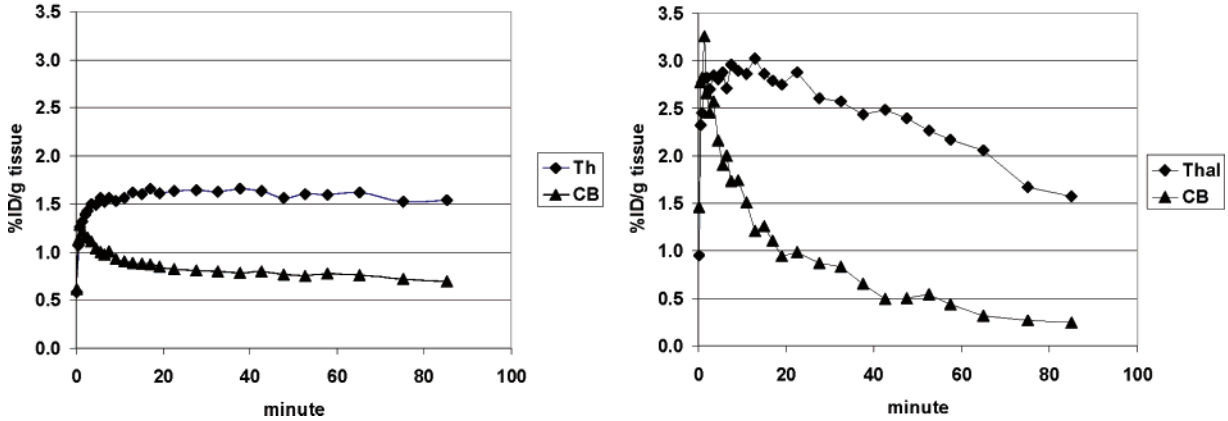

Figure 3. Baseline PET studies with [^{11}C](±)-**17** and [^{11}C](−)-**17** in rats. Top row: Transverse image of distribution of 0.3 mCi [^{11}C](−)-**17** in the brain of male Wistar rat (180 g). Legend: Ctx = cortex, Th = thalamus. Bottom row: Time-uptake curves of accumulation of radioactivity of [^{11}C](±)-**17** in the rat brain regions of a single animal (left) and [^{11}C](−)-**17** (right).

Scheme 3. Stereoselective Radiosynthesis of [^{11}C]-(±)-**17**, [^{11}C]-(−)-**17**, [^{11}C]-(+)-**24d**, and [^{11}C]-(−)-**24d**

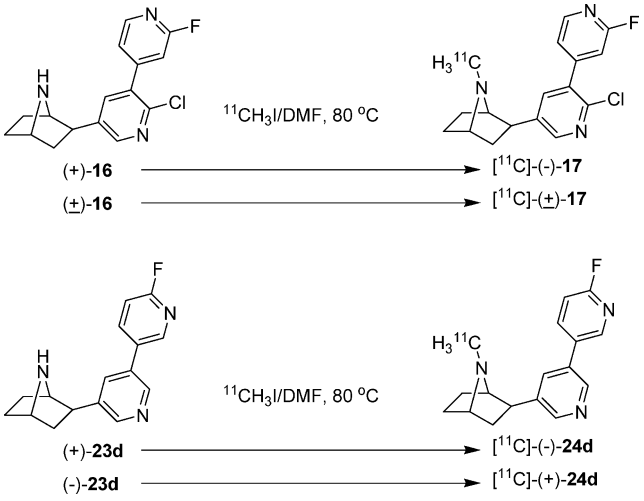

(±)-**16** and (+)-**16** with [^{11}C]-methyl iodide (Scheme 3). After HPLC purification, the final products [^{11}C]-(±)-**17** and [^{11}C]-(−)-**17** were free of nonlabeled contaminants, with an average nondecay corrected radiochemical yield of 19 ± 5% that was determined with respect to starting [^{11}C]methyl iodide. The average specific radioactivity of the final products [^{11}C]-(±)-**17** and [^{11}C]-(−)-**17** was 312 GBq/μmol (8428 mCi/μmol) determined at the end of synthesis, and radiochemical purity was greater than 97%. The total synthesis time was 35 min. The stereoselectivity of the radiosynthesis of enantiomer [^{11}C]-(−)-**17** was confirmed by the chiral HPLC analysis (see Supporting Information).

Enantiomers (+)-**24d** and (−)-**24d** were also radiolabeled with ^{11}C under the similar conditions (Scheme 3) using precursors (−)-**23d** and (+)-**23d**, respectively. These precursors

Scheme 4. Radiosynthesis of [^{18}F](−)-**24d**

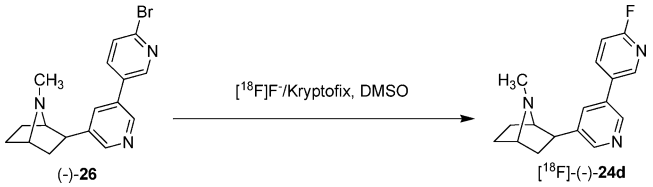

were prepared by chiral HPLC separation of racemic (±)-**23d** synthesized in this study (Table 2). Radiolabeled products [^{11}C]-(+)-**24d** and [^{11}C]-(−)-**24d** were obtained with radiochemical purities, specific radioactivities, and radiochemical yields similar to those of compounds [^{11}C]-(±)-**17** and [^{11}C]-(−)-**17**. The enantioselective nature of the methylation of (−)-**23d** and (+)-**23d** was confirmed by chiral HPLC analysis of the reaction products in separate experiments (see Supporting Information).

Radiofluorinated enantiomer [^{18}F](−)-**24d** was prepared with high yield, purity, and specific radioactivity by Kryptofix-assisted reaction of bromo derivative (−)-**26** with [^{18}F]fluoride under the conditions described elsewhere[19] (Scheme 4). The high enantiomeric purity of [^{18}F](−)-**24d** was confirmed by chiral radio-UV HPLC analysis (see Supporting Information).

In Vivo Studies. Novel compound [^{11}C](±)-**17** prepared initially in this study and having optimal lipophilicity for BBB permeability and binding affinity equal to that of epibatidine (Table 2) and its active enantiomer [^{11}C](−)-**17** were studied here as potential radioligands for imaging of central nAChR in Wistar male rats using small animal PET. Both radioligands displayed rapid accumulation of radioactivity in the rat brain in the baseline experiments (Figure 3). The pattern of radioactivity distribution in the rat brain is comparable to the distribution of nAChRs that was found in the previous autoradiographic[20] and PET experiments.[21] In the Th, a region with highest density of nAChR in the rat brain, both radioligands, [^{11}C](±)-

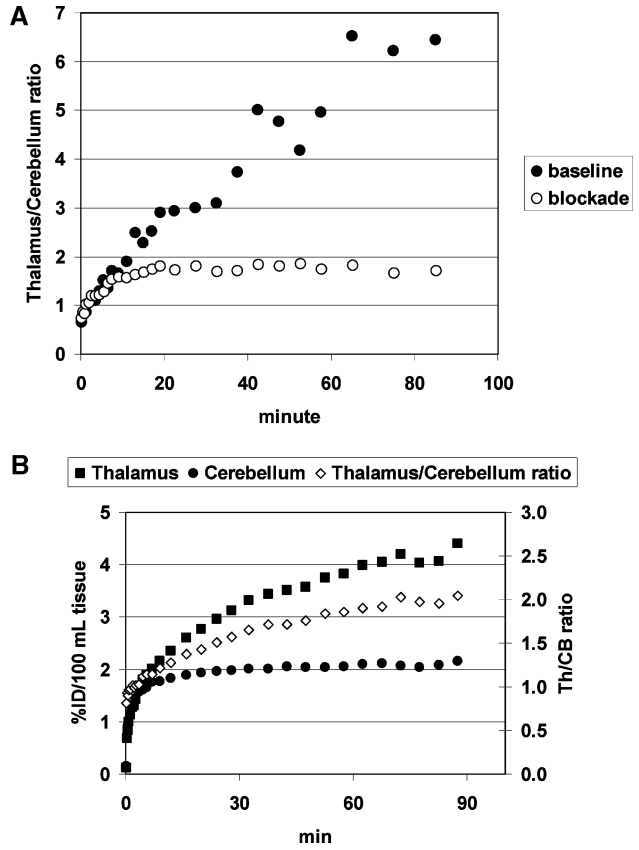

Figure 4. (A) Thalamus/cerebellum ratio of accumulated radioactivity vs time in the baseline and blockade (1 mg/kg cytisine, i.p., 5 min prior to injection of the radiotracer) PET experiments with [^{11}C](−)-**17** in a single rat. (B) Regional distribution of [^{11}C](−)-**17** in the baboon brain (single PET scan).

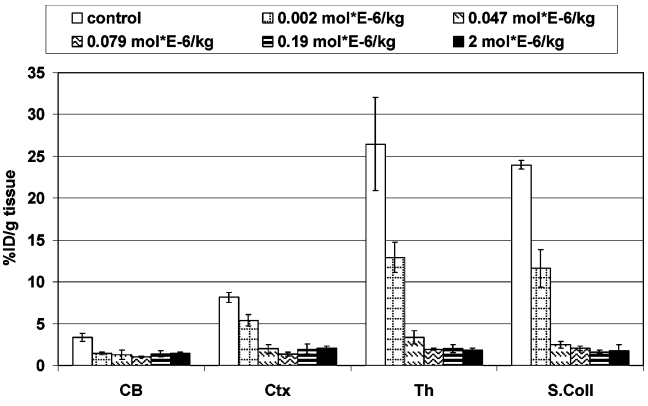

Figure 5. Blockade of accumulation of radioactivity (60 min time point) of [^{11}C](−)-**24d** in the mouse brain regions after intravenous administration of various doses of (−)-**24d** in CD-1 male mice (three animals).

17 and [^{11}C](−)-**17**, reached the maximum accumulation of radioactivity (1.7%ID/g tissue and 3.0%ID/g tissue, respectively) at 10−15 min postinjection. In the cerebellum (CB), a region with the lowest density of nAChRs, both radioligands manifested very rapid uptake, with a maximum at 1 min postinjection followed by rapid washout. The Th-to-CB ratio, a parameter that reveals the contrast between nAChR-rich and nAChR-poor regions in PET images, increased over the 90 min observation period, reaching values of 6.5 ([^{11}C](−)-**17**) and 2.2 ([^{11}C](±)-**17**). The higher Th/CB ratio of enantiomer [^{11}C](−)-**17** versus racemate [^{11}C](±)-**17** is in accord with greater binding affinity of the enantiomer.

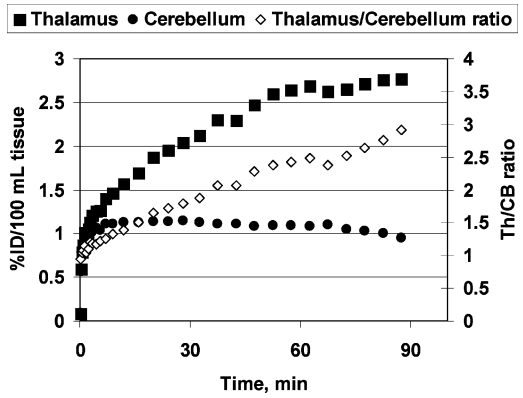

Figure 6. Regional distribution of the high affinity enantiomer [^{11}C]-(−)-**24d** in the baboon brain (single PET scan).

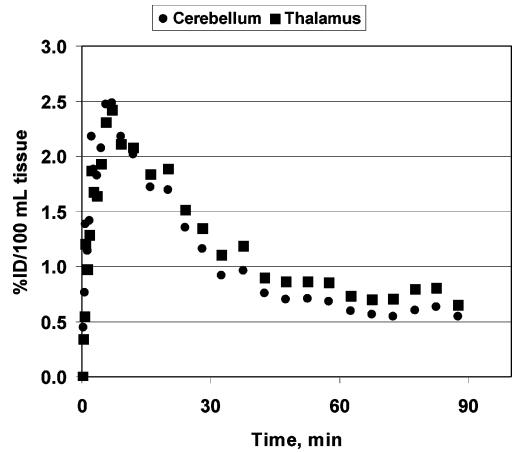

Figure 7. Regional distribution of the low affinity enantiomer [^{11}C]-(+)-**24d** in the baboon brain (single PET scan).

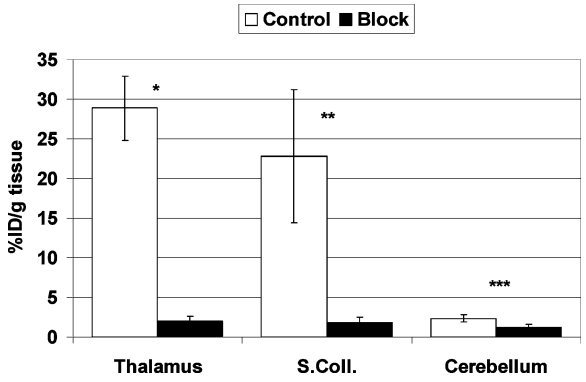

Figure 8. Comparison of the regional brain uptake of [^{18}F](−)-**24d** in CD1 male mice at the 60 min time point in control (three animals; white bars) and blocking (three animals) experiments with α4β2-nAChR ligand cytisine (black bars, 5 mg/kg, s.c.). There was significant blocking in the nAChR-rich thalamus, and superior colliculus and insignificant blocking in the nAChR-poor cerebellum. Data are means ± SD. *$p = 0.001$ and **$p = 0.02$, significantly different from controls; ***$p = 0.06$, insignificantly different from controls (ANOVA single factor analysis).

In the blocking experiments with [^{11}C](−)-**17**, pre-administration of cytisine (1 mg/kg, i.p.), a selective α4β2-nAChR ligand, dramatically reduced the regional radioactivity uptake in the rat Th, whereas little displacement of radioactivity from the nAChR-poor CB was observed. As a result, the Th/CB ratio in the blockade study was substantially lower (1.8) than that in the baseline study (6.5; Figure 4A). This blocking study suggests that [^{11}C](−)-**17** uptake in the receptor-rich regions of the brain is nAChR-mediated.

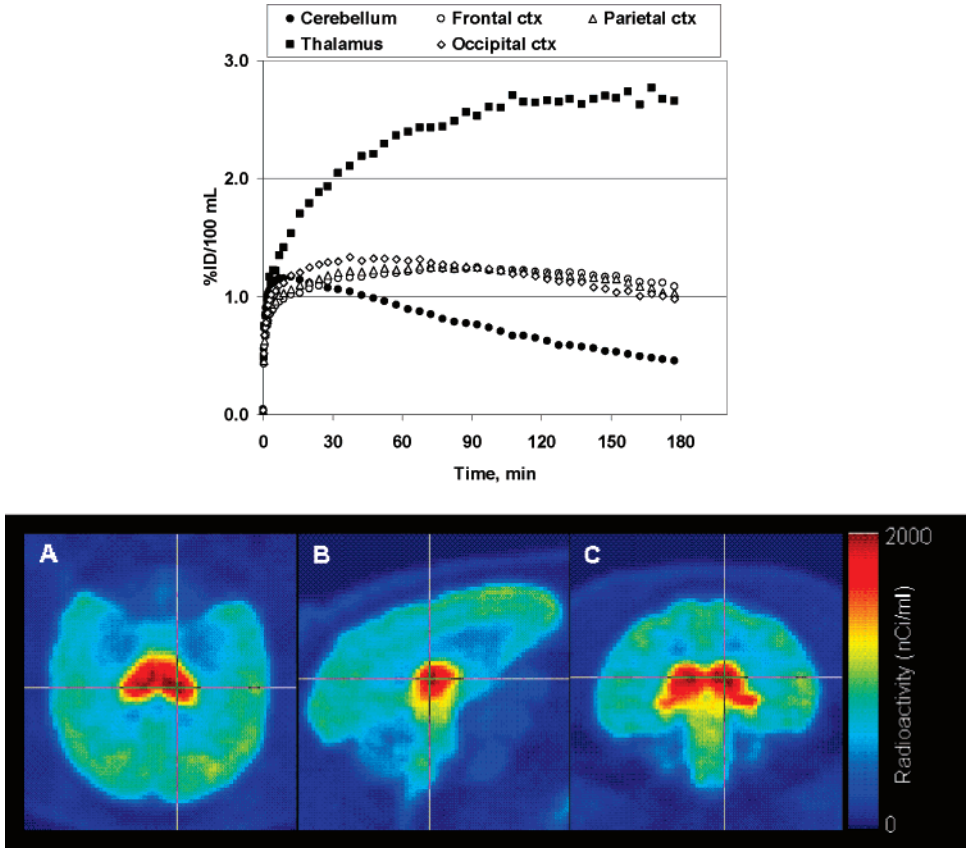

Figure 9. Top: Regional distribution of [^{18}F](−)-**24d** in the baboon brain (single PET scan). Bottom: Baboon PET, mean of 20−180 min frames. *trans*-Axial (panel A), sagittal (B), and coronal (C) radioactivity images. Crosshairs indicate positions of the three orthogonal images (center = right thalamus). The images also show relatively high accumulations in cortical mantle (A, B, and C) and pons (C).

Based on the favorable outcome with [^{11}C](−)-**17** in rats, PET studies in baboons were performed and showed an appropriate regional distribution of [^{11}C](−)-**17** in a baboon brain matching the distribution of nAChR (Figure 4B). However, the substantial accumulation of radioactivity in the nAChR-poor CB suggested high nonspecific binding (Th/CB ratio = 2 at 90 min postinjection) that can be explained by a relatively high lipophilicity of **17** (Table 2). Other PET nAChR-radioligands, like 2-[^{18}F]-FA and 6-[^{18}F]FA exhibit substantially lower lipophilicity and, correspondingly, low nonspecific binding.[3] These results suggested that another high affinity radioligand of this series, [^{11}C]-(−)-**24d**, having lower lipophilicity (Table 2) than that of [^{11}C](−)-**17**, might demonstrate lower nonspecific binding and better signal-to-noise ratios.

Preliminary baseline experiments with [^{11}C](−)-**24d** in mice and blockade experiments with nonradiolabeled (−)-**24d** showed that the radioligand labels nAChR in the mouse brain with remarkably high uptake (Figure 5). The specific binding of [^{11}C]-(−)-**24d** in the Th amounted to 94% when the blocked (by preadministration of nonlabeled (−)-**24d**) CB was used as a measure of nonspecific binding. Importantly, blocking doses of 0.002−0.2 μmol/kg intravenously injected (−)-**24d** did not produce noticeable pharmacological effects in mice. The highest injected dose (2 μmol/kg) of (−)-**24d** induced in animals fast breathing and Straub tail, but no death. Therefore, the acute toxic properties of (−)-**24d** in mice appear to be moderate and comparable with those for 2-[^{18}F]FA[22] and 6-[^{18}F]FA,[23] the radioligands that are currently used for human studies. The low toxic profile of **24d** is in agreement with experiments of other workers demonstrated that many congeners of **24d** are antagonists or partial agonists of nAChR.[9,10,13]

As expected, in the baboon PET experiments, [^{11}C](−)-**24d** showed lower uptake in the CB and high accumulation in the Th (Figure 6) and, therefore, a better signal-to-noise ratio as compared to [^{11}C](−)-**17**. In contrast, a PET experiment with a low binding affinity enantiomer [^{11}C](+)-**24d** did not demonstrate any considerable specific binding of the radioligand in the baboon brain (Figure 7). It is noteworthy that initial peak uptake of high affinity enantiomer [^{11}C]-(−)**24d** was lower than that of lower affinity enantiomer [^{11}C]-(+)**24d**. The statistical significance and mechanism for this phenomenon remain to be elucidated in the future studies. PET modeling experiments (data not presented) suggest that by the end of a 90-min scan, radioligand [^{11}C](−)-**24d** did not reach a steady-state in the baboon brain (Figure 6). PET scanning of ^{11}C-radioligands is limited to 90−100 min due to their half-life ($t_{1/2}$ = 20 min). To get an extended scan (120−180 min), (−)-**24d** was radiolabeled with ^{18}F (see above).

Initial baseline and blocking studies with $\alpha 4\beta 2$-nAChR ligand cytisine in mice with [^{18}F](−)-**24d** demonstrated that the radioligand specifically labels nAChR in the mouse brain regions (Figure 8).

The PET experiment in baboon (Figure 9) showed that [^{18}F]-(−)-**24d** displayed high accumulation of radioactivity in nAChR-rich brain regions. The tissue-to-CB ratios of [^{18}F](−)-**24d** reached values of 6, 2.4, and 2.4 at 180 min postinjection in the Th, pons, and the frontal cortex, respectively. These ratios are about 250−300% as great as those of 2-[^{18}F]FA and 6-[^{18}F]-FA, the only available radioligands for studying nAChR in human subjects. The radiotracer kinetics in baboon cortexes reached a steady-state at 120 min postinjection (PET modeling analysis is not presented).

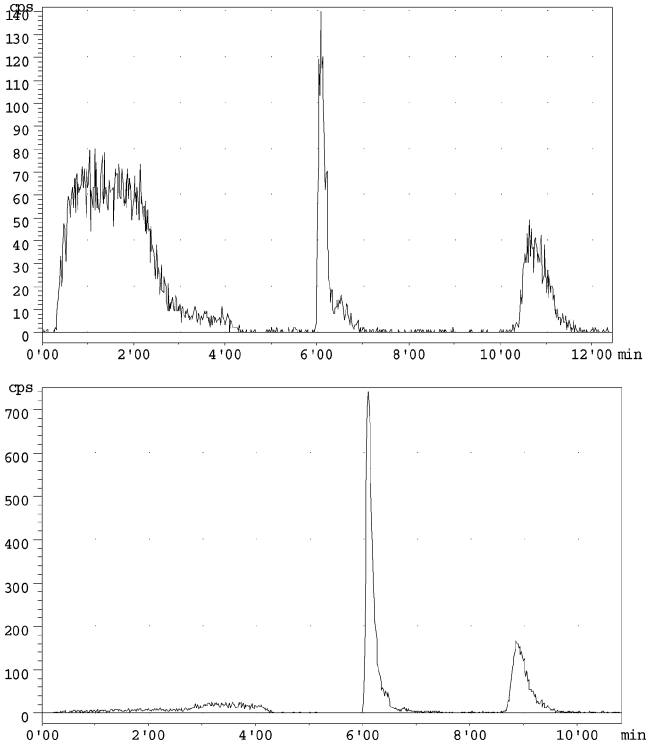

Figure 10. HPLC analysis of radiolabeled metabolites in baboon plasma 30 min post administration of radioligand. Top: [^{11}C](−)-**24d**; bottom: [^{18}F](−)-**24d**.

HPLC analysis of metabolites of [^{11}C]-(−)-**24d** and [^{18}F]-(−)-**24d** in baboon plasma was performed. There was only one major metabolite of [^{18}F]-(−)-**24d** observed at 30 min postinjection. At the same 30 min time point, [^{11}C](−)-**24d** had two major metabolites with prevalence of the HPLC peak that was not seen in the [^{18}F]-(−)-**24d** metabolism study (Figure 10). This striking difference in the radiolabeled metabolites could be a reason of some dissimilarity between the time-uptake curves of [^{11}C]-(−)-**24d** (Figure 6) and [^{18}F]-(−)-**24d** (Figure 9).

Conclusion

A novel series of high affinity nAChR ligands, derivatives of racemic 7-methyl-2-(5-(pyridinyl)pyridin-3-yl)-7-azabicyclo-[2.2.1]heptane and its enantiomers, has been developed. In vitro inhibition binding assays demonstrated considerable enan tioselectivity of (−)-7-methyl-2-(5-(pyridinyl)pyridin-3-yl)-7-azabicyclo[2.2.1]heptane derivatives as nAChR ligands. In vivo enantioselectivity of (−)-7-methyl-2-(5-(pyridinyl)pyridin-3-yl)-7-azabicyclo[2.2.1]heptane derivatives radiolabeled with positron-emitting isotopes was observed in biodistribution studies in rodents and baboon.

One of the radiolabeled compounds developed here, [^{18}F]-(−)-**24d**, potentially manifests good properties for imaging of ET nAChR. In vivo studies with [^{18}F](−)-**24d** confirmed that the compound specifically labels nAChR in the mouse brain. Preliminary evaluation of [^{18}F](−)-**24d** in a single baboon PET experiment demonstrated distribution of radioactivity that matches known distribution of nAChR receptors, high target-to-nontarget ratio in nAChR-rich Th and a respectful ratio in the regions with intermediate density of nAChR (cortex and pons) and relatively rapid brain kinetics. Further preclinical evaluations of [^{18}F](−)-**24d**, including PET modeling and determination of radiometabolites in the brain, blockade and test/retest PET experiments in baboon, radiation dosimetry, and pre-IND toxicology, are warranted in future studies.

Experimental Section

Chemicals were obtained from Aldrich (Milwaukee, WI) and used as received. Column chromatography was carried out using E. Merck silica gel 60F (230−400 mesh). Analytical thin-layer chromatography (TLC) was performed on aluminum sheets coated with silica gel 60 F_{254} (0.25 mm thickness, E. Merck, Darmstadt, Germany). Melting points were determined with a Fisher-Johns apparatus and are not corrected. ^{1}H NMR and ^{13}C NMR spectra were recorded with a Varian-400 NMR spectrometer at nominal resonance frequencies of 400 and 100 MHz, respectively, in $CDCl_3$ (referenced to internal Me_4Si at δ_H 0 ppm, δ_C 0 ppm). The chemical shifts (δ) were expressed in parts per million (ppm). First order J values were given in Hertz. High-resolution mass spectrometry was performed at the University of Notre Dame Mass Spectrometry facility. Elemental analyses were determined by Galbraith Laboratories, Inc. (Knoxville, TN). The HPLC system consisted of two Waters model 590EF pumps, two Rheodyne model 7126 injectors, an in-line Waters model 441 UV detector (254 nm), and a single sodium iodide crystal flow radioactivity detector. All HPLC chromatograms were recorded with Varian Galaxie software (version 1.8). The analytical and semipreparative chromatography were performed using Phenomenex Luna C-18 10 μm columns (analytical 4.6 × 250 mm and semipreparative 10 × 250 mm). The racemic compounds were separated into their enantiomers by chiral HPLC using a Chiralcel-OD column, 250 × 20 mm (Daicel Chemical Industries, Ltd.) and a mixture of 2-propanol/hexane/triethylamine, as an eluent, at a flow rate of 4 mL/min. A dose calibrator (Capintec 15R) was used for all radioactivity measurements. [^{11}C]Methyl iodide was prepared using a General Electric Methyl Iodide Microlab from [^{11}C]carbon dioxide produced by General Electric PETtrace biomedical cyclotron. Radiofluorination was performed with modified GE FDG radiochemistry box.

7-*tert*-Butoxycarbonyl-2-*exo*-(3′-bromo-2′-chloro-5′-pyridinyl)-7-azabicyclo[2.2.1]heptane (14). Compound **13**[14] (150 mg, 0.52 mmol) was dissolved in anhydrous THF (3 mL) at room temperature. Di-*tert*-butyldicarbonate (227 mg, 1.05 mmol, 2 equiv) was added, and the reaction mixture was heated to reflux for 12 h. The solvent was removed by evaporation, and the residue was purified by flash column chromatography (Hex/EtOAc 4:1) to provide the product as a colorless syrup (168 mg, 83%). ^{1}H NMR 8.21 (d, J = 2.4 Hz, 1H), 7.93 (d, J = 2.0 Hz, 1H), 4.39 (br s, 1H), 4.18 (br s, 1H), 2.86 (dd, J = 4.4 Hz, 8.8 Hz, 1H), 2.01(dd, J = 8.8 Hz, 12.4 Hz, 1H), 1.85 (br s, 3H), 1.51−1.60 (m, 2H), 1.45 (s, 9H). HRMS calcd for $C_{16}H_{21}BrClN_2O_2$ [M + H] m/z, 387.0475; found, 387.0457.

7-*tert*-Butoxycarbonyl-2-*exo*-[2′-chloro-3′-(2-fluoropyridin-4-yl)-5′-pyridinyl]-7-azabicyclo[2.2.1]heptane (15). Compound **14** (123 mg, 0.32 mmol), 2-fluoro-4-trimethyltinpyridine[4] (113 mg, 0.43 mmol, 1.36 equiv), and tetrakis(triphenylphosphine)palladium-(0) (23.8 mg, 0.021 mmol) were dissolved in anhydrous toluene (3 mL). The mixture was heated in a sealed reaction vessel and stirred at 115−120 °C for 9 h. TLC (1:1 hexanes/ethyl acetate) was used to monitor the reaction process. The solvent was then evaporated at 50−60 °C. Final purification was done by gradient flash column chromatography (5:1 to 3:2 hexane/ethyl acetate). The product **15** (103 mg) was obtained with 80% yield. ^{1}H NMR (400 MHz, $CDCl_3$/TMS) δ 8.35 (d, J = 2.4 Hz, 1H), 8.31 (d, J = 4.8 Hz, 1H), 7.68 (d, J = 2.4 Hz, 1H), 7.31 (m, 1 H), 7.04 (s, 1H), 4.39 (br s, 1H), 4.22 (br s, 1H), 2.94 (dd, J = 8.8 Hz, 5.2 Hz, 1H), 2.05 (m, 1H), 1.82−1.86 (m, 3H), 1.54−1.63 (m, 2H), 1.41 (s, 9 H). HRMS calculated for $C_{21}H_{24}ClFN_3O_2$ [M + H] m/z, 404.1541; found, 404.1534.

(±)-2-*exo*-[2′-Chloro-3′-(2-fluoropyridin-4-yl)-5′-pyridinyl]-7-azabicyclo[2.2.1]heptane ((±)-16). A solution of 96 mg (0.24 mmol) of **15** in CH_2Cl_2 (3 mL) and trifluoroacetic acid (0.32 mL) was allowed to stir at room temperature for 1.5 h. The organic solvents were removed by evaporation. The residue was purified by silica gel column chromatography using $CHCl_3$/EtOH 15:1 as eluent to give 173 mg of product **16** (94%). TFA salt: ^{1}H NMR 8.40 (d, J = 2.8 Hz, 1H), 8.26 (d, J = 5.2 Hz, 1H), 7.84 (d, J =

2.4 Hz, 1H), 7.34 (m, 1H), 7.07 (br s 1H), 4.36 (d, $J = 4.0$ Hz, 1H), 4.31 (d, $J = 4.0$ Hz), 3.28 (m, 1H), 2.15−2.39 (m, 5H), 1.73−1.91 (m, 2H). Free base: ^{1}H NMR 8.38 (d, $J = 2.4$ Hz, 1H), 8.30 (d, $J = 5.2$ Hz, 1H), 7.86 (d, $J = 2.4$ Hz, 1H), 7.32 (m, 1H), 7.05 (br s, 1H), 3.81 (s, 1H), 3.59 (s, 1H), 2.81 (m, 1H), 1.91 (m, 1H), 1.54−1.66 (m, 6H). HRMS calcd for $C_{16}H_{16}ClFN_3$ [M + H] *m*/*z*, 304.1017; found, 304.1016. Anal. ($C_{16}H_{15}ClFN_3 \cdot 3.75TFA \cdot 2H_2O$) C, H, N.

7-Methyl-2-*exo*-[2′-chloro-3′-(2-fluoropyridin-4-yl)-5′-pyridinyl]-7-azabicyclo[2.2.1]heptane (17). A mixture of the secondary amine **16** (TFA salt, 60 mg, 0.08 mmol) and 37% formaldehyde (0.052 mL, 0.65 mmol) in acetonitrile (3 mL) was stirred for 20 min at room temperature, after which sodium cyanoborohydride (15.3 mg, 0.24 mmol) was added in small portions. Stirring was continued for 12 h. The solvent was evaporated at reduced pressure and 15 mL of 2% K_2CO_3 solution was added to the residue. The resulting mixture was extracted with three 20 mL portions of $CHCl_3$. The combined $CHCl_3$ extracts were washed with 10 mL water, dried with anhydrous Na_2SO_4, and evaporated in vacuo to give a reside. After purification by column chromatography on silica gel with CH_2Cl_2/MeOH (15:1), the product was obtained as a colorless oil (33 mg). ^{1}H NMR (400 MHz, $CDCl_3$/TMS) δ 8.40 (d, $J = 2.4$ Hz, 1H), 8.32 (dd, $J = 4.8$ Hz, 0.8 Hz, 1H), 7.92 (d, $J = 2.0$ Hz, 1H), 7.32 (m, 1 H), 7.05 (m, 1H), 3.34 (m, 1H), 3.15 (d, $J = 4.0$ Hz, 1H), 2.72 (dd, $J = 9.2$ Hz, 4.8 Hz), 2.24 (s, 3H), 1.86−1.97 (m, 2H), 1.68−1.73 (m, 2H), 1.44 (m, 2 H). HRMS calcd for $C_{17}H_{18}ClFN_3$ [M + H] *m*/*z*, 318.1173; found, 318.1162. Anal. ($C_{17}H_{17}ClFN_3 \cdot 0.5H_2O$) C, H, N.

General Procedures for Suzuki Coupling Reactions (Compounds 22a, 22b, and 22c). To a resealable reaction vessel under nitrogen were added (0.896 mmol) the bromo derivative (**18** or **19**), $Pd(OAc)_2$ (20 mg, 0.0896 mmol), P(*o*-tolyl)$_3$ (55 mg, 0.179 mmol), sodium carbonate (192 mg, 1.79 mmol), boronic acid (**20** or **21**; 1.434 mmol, 1.6 equiv), degassed (nitrogen bubbling) water (0.7 mL), and dimethoxyethane (DME, 6 mL). The reaction was heated at 80 °C for 5 h, cooled, poured into 40 mL of saturated $NaHCO_3$, and extracted with EtOAc (4 × 30 mL). The solvent was then evaporated at 50−60 °C. Final purification of compounds **22a**, **22b**, and **22c** has been done by flash chromatography ($CHCl_3$/MeOH/Et_3N 15:1:0.5).

7-*tert*-Butoxycarbonyl-2-*exo*-[2′-amino-3′-(6-fluoropyridin-3-yl))-5′-pyridinyl]-7-azabicyclo[2.2.1]heptane (22a). The reagents were compounds **18**[24] and **20**. The yield is 87%. ^{1}H NMR (400 MHz, $CDCl_3$/TMS) δ 8.30 (m, 1H), 7.99 (d, $J = 2.4$ Hz, 1H), 7.90 (ddd, $J = 2.4$ Hz, 8.0 Hz, 16 Hz, 1H), 7.35 (d, $J = 2.4$ Hz, 1H), 7.03 (dd, $J = 3.2$ Hz, 7.6 Hz, 1H), 4.42 (br s, 2H), 4.36 (br s, 1H), 4.15 (m, 1H), 2.81 (m, 1H), 1.96 (dd, $J = 8.8$ Hz, 12.4 Hz, 1H), 1.84 (m, 3H), 1.52−1.61 (m, 2H), 1.49 (s, 9H). HRMS calcd for $C_{21}H_{26}FN_4O_2$ [M + H] *m*/*z*, 385.2040; found, 385.2025.

7-*tert*-Butoxycarbonyl-2-*exo*-[2′-amino-3′-(6-cyanopyridin-3-yl))-5′-pyridinyl]-7-azabicyclo[2.2.1]heptane (22b). The reagents were compounds **18**[24] and **21**. The yield is 74%. ^{1}H NMR (400 MHz, $CDCl_3$/TMS) δ 8.84 (m, 1H), 8.03 (d, $J = 2$ Hz, 1H), 7.99 (dd, $J = 2.0$ Hz, 8.0 Hz, 1H), 7.78 (dd, $J = 0.8$ Hz, 8.4 Hz, 1H), 7.39 (d, $J = 2.0$ Hz, 1H), 4.46 (s, 2H), 4.35 (br s, 1H), 4.15 (s, 1H), 2.82 (dd, $J = 5$ Hz, 8.6 Hz, 1H), 1.98 (dd, $J = 9.4$ Hz, 12.6 Hz, 1H), 1.83 (br s, 3H), 1.50−1.61 (m, 2H), 1.40 (s, 9H). HRMS calculated for $C_{22}H_{26}N_5O_2$ [M + H] *m*/*z*, 392.2086; found, 392.2094.

7-*tert*-Butoxycarbonyl-2-*exo*-[3′-(6-fluoropyridin-3-yl))-5′-pyridinyl]-7-azabicyclo[2.2.1]heptane (22c). The reagents were compounds **19**[25] and **20**. The yield is 83%. ^{1}H NMR (400 MHz, $CDCl_3$/TMS) δ 8.64 (d, $J = 2.4$ Hz, 1H), 8.53 (d, $J = 2.0$ Hz, 1H), 8.42 (d, $J = 2.8$ Hz, 1H), 7.99 (m, 1H), 7.84 (m, 1H), 7.04 (dd, $J = 2.8$ Hz, 8.8 Hz, 1H), 4.42 (br s, 1H), 4.27 (br s, 1H), 2.97 (dd, $J = 4.8$ Hz, 8.8 Hz, 1H), 2.06 (dd, $J = 9.2$ Hz, 12.4 Hz, 1H), 1.88 (m, 3H), 1.55−1.61 (m, 2H), 1.43 (s, 9H). HRMS calcd for $C_{21}H_{25}FN_3O_2$ [M + H] *m*/*z*, 370.1931; found, 370.1950.

2-*exo*-[2′-Chloro-3′-(6-fluoropyridin-3-yl)-5′-pyridinyl]-7-azabicyclo[2.2.1]heptane (23a). Precursor **22a** (160 mg, 0.436 mmol) was added under stirring to 2.8 mL of 36% hydrochloric acid at 0 °C, and 756 mg (10.9 mmol) of $NaNO_2$ was added at 0 °C in small portions over 10 min. The mixture was stirred for 15 min at 0 °C, then 862 mg (8.74 mmol) of CuCl was added in small portions over 30 min as solid and stirred at 0 °C for 30 min. After 1 h of stirring at room temperature, the reaction mixture was poured into 80 mL of 1:1 NH_4OH and H_2O and extracted with 4 × 50 mL of $CHCl_3$. The combined organic phase was dried (Na_2SO_4), filtered, and concentrated under reduced pressure to give a residue, which was purified by $CHCl_3$/MeOH 15:1 to give **23a** as an oil (77 mg, 58%). ^{1}H NMR (400 MHz, $CDCl_3$/TMS) δ 8.35 (d, $J = 2.0$ Hz, 1H), 8.29 (m, 1H), 7.91−7.96 (m, 1H), 7.85 (d, $J = 2.4$ Hz, 1H), 7.03 (dd, $J = 2.8$ Hz, 8.8 Hz, 1H), 3.81 (s, 1H), 3.61 (s, 1H), 2.81 (m, 1H), 1.92−1.97 (m, 1H), 1.55−1.69 (m, 5H). ^{13}C NMR (100 MHz, $CDCl_3$/TMS) δ 164.73, 162.33, 148.83, 148.26, 148.10, 147.49, 142.51, 142.43, 142.37, 138.93, 132.15, 131.94, 131.89, 109.57, 109.20, 63.09, 56.63, 44.63, 40.76, 31.83, 30.61.

2-*exo*-[2′-Fluoro-3′-(6-fluoropyridin-3-yl)-5′-pyridinyl]-7-azabicyclo[2.2.1]heptane (23b). A solution of 62 mg (0.161 mmol) of **22a** in 70% HF−pyridine (1.5 mL) inside a plastic reaction vessel was allowed to stir at 0 °C for 30 min. Sodium nitrite (116 mg, 1.67 mmol) was then added in small portions and stirring was continued at room temperature for 1 h. The mixture was then poured into a solution of 1:1 NH_4OH/H_2O (40 mL) and extracted with ethyl acetate. The combined organic layers were dried with magnesium sulfate and concentrated, and then the residue was purified via flash chromatography on silica gel using $CHCl_3$/MeOH 10:1 to 2:1 to furnish product **23b** (40 mg, 86%) as a colorless oil. ^{1}H NMR (400 MHz, $CDCl_3$/TMS) δ 8.43 (br s, 1H), 8.13 (br s, 1H), 8.0−8.08 (m, 2H), 7.03−7.06 (m, 1H), 3.84 (br s, 1H), 3.64 (s, 1H), 2.86 (dd, $J = 4.4$ Hz, 8.8 Hz, 1H), 2.11 (s, 3H), 1.96 (dd, $J = 9.2$ Hz, 12 Hz 1H), 1.57−1.67 (m, 4H).

2-*exo*-2′-Fluoro-3′-(6-cyanopyridin-3-yl))-5′-pyridinyl]-7-azabicyclo[2.2.1]heptane (23c). A solution of 96 mg (0.245 mmol) of **22b** in 70% HF−pyridine (2.3 mL) in a plastic reaction vessel was allowed to stir at 0 °C for 30 min. Sodium nitrite (178 mg, 2.58 mmol) was then added in small portions and stirring was continued at room temperature for 1 h. The mixture was then poured into a solution of 1:1 NH_4OH/H_2O (60 mL) and extracted with ethyl acetate. The combined organic layers were dried with magnesium sulfate and concentrated, and then the residue was purified via flash chromatography on silica gel using $CHCl_3$/MeOH 8:1 to 3:1 to furnish **23c** (56%) as a colorless oil. ^{1}H NMR (400 MHz, $CDCl_3$/TMS) δ 8.94 (s, 1H), 8.17−8.19 (m, 2H), 8.07−8.10 (m, 1H), 7.81 (dd, $J = 0.8$ Hz, 8.0 Hz, 1H), 3.85 (br s, 1H), 3.62 (s, 1H), 2.85 (m, 1H), 1.86 (m, 2H), 1.58−1.70 (m, 5H). Anal. ($C_{17}H_{15}FN_4 \cdot 0.35H_2O$) C, H, N.

2-*exo*-[3′-(6-Fluoropyridin-3-yl)-5′-pyridinyl]-7-azabicyclo-[2.2.1]heptane (23d). A solution of 86 mg (0.24 mmol) of **22c** in CH_2Cl_2 (3 mL) and trifluoroacetic acid (0.32 mL) was allowed to stir at 0 °C to room temperature for 12 h. The organic solvents were removed by evaporation. The residue was purified by silica gel column chromatography using $CHCl_3$/EtOH 10:1 to 2:1 as eluent to give 73 mg of product (60%). ^{1}H NMR (400 MHz, $CDCl_3$/TMS) δ 8.62 (d, $J = 2.0$ Hz, 1H), 8.57 (d, $J = 2.0$ Hz, 1H), 8.43 (d, $J = 2.4$ Hz, 1H), 8.00 (m, 1H), 7.96 (m, 1H), 3.84 (m, 1H), 3.66 (s, 1H), 2.88 (dd, $J = 5.0$ Hz, 9 Hz), 1.97 (dd, $J = 12.4$ Hz, 8.8 Hz, 1H), 1.74 (m, 2H), 1.56−1.66 (m, 3H). Anal. ($C_{16}H_{16}FN_3 \cdot 2CF_3COOH \cdot 0.5\ H_2O$) C, H, N.

General Procedures for Preparing Tertiary Amines 24a−d. The secondary amine **23a−d** (0.14 mmol) was dissolved in 1 M sodium phosphite solution (2.5 mL). Aqueous formaldehyde (37%) (0.22 mL) was added, and the reaction mixture was heated with stirring at 60 °C for 30 min in an oil bath. The reaction flask was cooled and 5% K_2CO_3 (25 mL) was added. The mixture was extracted with $CHCl_3$ (4 × 20 mL). The $CHCl_3$ extracts were dried over sodium sulfate, filtered, and evaporated to give a residue that was purified by silica gel chromatography ($CHCl_3$/MeOH 10:1 to 5:1), revealing tertiary amines **24a−d**.

7-Methyl-2-*exo*-[2′-chloro-3′-(6-fluoropyridin-3-yl)-5′-pyridinyl]-7-azabicyclo[2.2.1]heptane (24a). The reagent was compound **23a.** The product was obtained as a colorless oil (42 mg, 84%). ^{1}H

NMR (400 MHz, $CDCl_3$/TMS) δ 8.37 (d, $J = 2.4$ Hz, 1H), 8.29 (m, 1H), 7.95 (m, 1H), 7.91 (d, $J = 2.0$ Hz, 1H), 7.04 (m, 1H), 3.33 (m, 1H), 3.17 (m, 1H), 2.72 (m, 1H), 2.24 (s, 3H), 1.91−1.96 (m, 2H), 1.69 (br s, 2H), 1.45 (m, 2H). HRMS calcd for $C_{17}H_{18}ClFN_3$ [M + H] *m*/*z*, 318.1173; found, 318.1158.

7-Methyl-2-*exo*-[2′-fluoro-3′-(6-fluoropyridin-3-yl)-5′-pyridinyl]-7-azabicyclo[2.2.1]heptane (24b). The reagent was compound **23b**. The product was obtained as a white solid, mp 92−93 °C. The yield is 88%. ^{1}H NMR (400 MHz, $CDCl_3$/TMS) δ 8.41 (s, 1H), 8.13−8.16 (m, 2H), 8.03 (m, 1H), 7.03−7.06 (dd, $J = 8.5$ Hz, 3.0 Hz, 1H), 3.3−3.41 (m, 1H), 3.17 (m, 1H), 2.68−2.81 (m, 1H), 2.26 (s, 3H), 1.85−2.05 (m, 3H), 1.64−1.78 (m, 1H), 1.37−1.54 (m, 2H). HRMS calcd for $C_{17}H_{18}F_2N_3$ [M + H] *m*/*z*, 302.1469; found, 302.1456. Anal. ($C_{17}H_{17}F_2N_3 \cdot 0.75H_2O$) C, H, N.

(7-Methyl-2-*exo*-[2′-fluoro-3′-(6-cyanopyridin-3-yl))-5′-pyridinyl]-7-azabicyclo[2.2.1]heptane (24c). The reagent was compound **23c**. The product was obtained as a white solid, mp 128−130 °C. Yield 86%. ^{1}H NMR (400 MHz, $CDCl_3$/TMS) δ 8.93 (m, 1H), 8.23 (d, $J = 2.4$ Hz, 9.6 Hz, 2H), 8.20 (m, 1H), 8.08 (m, 1H), 7.80 (dd, $J = 0.8$ Hz, 8.4 Hz, 1H), 3.36 (m, 1H), 3.15 (d, $J = 4$ Hz, 1H), 2.75 (m, 1H), 2.26 (s, 3H), 1.88−1.97 (m, 2H), 1.68−1.72 (m, 2H), 1.44−1.52 (m, 2H). HRMS calcd for $C_{18}H_{18}FN_4$ [M + H] *m*/*z*, 309.1515; found, 309.1508. Anal. ($C_{18}H_{17}FN_4 \cdot 0.2\ H_2O$) C, H, N.

7-Methyl-2-*exo*-[3′-(6-fluoropyridin-3-yl))-5′-pyridinyl]-7-azabicyclo[2.2.1]heptane (24d). The reagent was compound **23d**. The product was obtained as a colorless oil. Yield 94%. ^{1}H NMR (400 MHz, $CDCl_3$/TMS) δ 8.60 (br s, 2H), 8.43 (d, $J = 2$ Hz, 1H), 8.05 (m, 1H), 7.98 (m, 1H), 7.05 (dd, $J = 2.4$ Hz, 8.2 Hz, 1H), 3.37 (m, 1H), 3.23 (d, $J = 3.6$ Hz, 1H), 2.75 (dd, $J = 4.8$ Hz, 9.2 Hz, 1H), 2.27 (s, 3H), 1.88−2.02 (m, 2H), 1.68−1.78 (m, 2H), 1.47 (m, 2H). Anal. ($C_{17}H_{18}FN_3 \cdot 0.25CHCl_3 \cdot 0.2\ H_2O$) C, H, N.

7-Methyl-2-*exo*-[3′-(6(1*H*)-pyridinone-3-yl))-5′-pyridinyl]-7-azabicyclo[2.2.1]heptane (25). Formic acid (0.8 mL) was added to the precursor **24d** (383 mg, 1.35 mmol), and the reaction mixture was stirred at 105 °C for 3 h. The reaction was cooled and quenched with water and 5% K_2CO_3, and the mixture was extracted with $CHCl_3$. The extract was dried over Na_2SO_4 and evaporated in vacuum, and the residue was purified by chromatography on silica gel ($CHCl_3$/MeOH 3:1 to 1:1) to give the product **25** as colorless oil (266 mg, 70%). ^{1}H NMR (400 MHz, $CDCl_3$/TMS) δ 8.51 (dd, $J = 7.6$ Hz, 2.0 Hz, 2H), 7.96 (m, 1H), 7.80 (dd, $J = 9.2$ Hz, 2.8 Hz, 1H), 7.68 (m, 1H), 6.74 (d, $J = 9.6$ Hz, 1H), 3.36 (m, 1H), 3.20 (br s, 1H), 2.73 (dd, $J = 9.2$ Hz, 4.8 Hz, 1H), 2.28 (s, 3H), 1.88−1.98 (m, 3H), 1.71−1.71 (m, 1H), 1.47 (m, 2H).

7-Methyl-2-*exo*-[3′-(6-bromopyridin-3-yl))-5′-pyridinyl]-7-azabicyclo[2.2.1]heptane (26). Phosphorus oxybromide (198 mg, 0.67 mmol, 1.72 equiv) was added to a solution of the precursor **25** (111 mg, 0.39 m mol) in toluene (1 mL), quinoline (0.08 mL), DMF (0.3 mL), and THF (0.5 mL) at room temperature. The reaction mixture was stirred at 120 °C for 3 h. The vigorous reaction was monitored by TLC ($CHCl_3$/MeOH 2:3). The reaction mixture was cooled. The supernatant was evaporated, poured on ice, neutralized with saturated $NaHCO_3$ solution, and extracted with $CHCl_3$ (4 × 20 mL). The organic layers were washed with water, dried with Na_2SO_4, filtered, and evaporated to give a yellow residue. The residue was purified by silica gel chromatography to give **25** as pale yellow solid (58 mg, 43%). Mp 112−114 °C.

General Procedures for Resolution of Racemic Compounds 16, 17, 23c,d, 24c,d, and 26. The racemic compounds **16**, **17**, **23c**,**d**, **24c**,**d**, and **26** were separated into their (+)- and (−)-enantiomers by chiral HPLC, using a 250 × 20 mm CHIRALCEL-OD column, 1.5 mg per injection, mobile phase is 2-propanol/hexane/triethylamine (Table 1) at a flow rate of 4 mL/min. The fractions were detected by UV ($\lambda = 254$ nm).

N-Methylation of normethyl enantiomers of (+)-**16**, (−)-**16**, (+)-**23c**, (−)-**23c**, (+)-**23d**, and (−)-**23d**. The pure enantiomer (either (+)-**16**, (−)-**16**, (+)-**23c**, (−)-**23c**, (+)-**23d**, or (−)-**23d**; 1 mg) was dissolved in a solution of CH_3I (0.5 μL) in anhydrous DMF (100 μL) and the mixture was heated at 80 °C for 5 min and was diluted with 2-propanol/hexane (50:50, 0.5 mL). Chiral HPLC analysis of the reaction mixture was performed by injecting 50 μL of the mixture onto Chiralcel HPLC column (the eluents are shown in the Table 1). The products resulted from (+)-**16**, (+)-**23c**, and (+)-**23d** are identical to (−)-**17**, (−)-**24c**, and (−)-**24d**, which were obtained by semipreparative separation of racemates **17**, **24c**, and **24d**, respectively. The products prepared by methylation of (−)-**16**, (−)-**23c**, (−)-**23d** are identical to (+)-**17**, (+)-**24c**, and (+)-**24d**, which were obtained similarly from **17**, **24c**, and **24d**, respectively.

Radiochemistry. 7-[^{11}C]Methyl-2-*exo*-[2′-chloro-3′-(2-fluoropyridin-4-yl)-5′-pyridinyl]-7-azabicyclo[2.2.1]heptane (±)-17 or (−)-17. Precursor (±)-**16** or (−)-**16** (1 mg) was dissolved in 200 μL of anhydrous DMF, capped in a small V-vial and cooled to −40 °C. [^{11}C]Methyl iodide was swept by argon flow into the vial. After the radioactivity reached a plateau, the vial was assayed in the dose calibrator and then heated at 80 °C for 5 min. Water (200 μL) was added, and the solution was injected onto the semipreparative HPLC column (Phenomenex Luna C-18 10 μm column, semipreparative 10 × 250 mm, 46:54:0.1 v/v/v CH_3CN/0.1 M ammonium formate/triethylamine (TEA), 12 mL/min). The retention time of normethyl precursor **16** was 3.5 min. The product peak, having a retention time of 8.7 min, was collected in 50 mL of HPLC water. The water solution was transferred through a Waters C-8 Sep-Pak Plus. The product was eluted with 1 mL ethanol into a vial and diluted with 9 mL of 0.9% saline. The final product [^{11}C]-**17** was then analyzed by analytical HPLC (Phenomenex Luna C-18 10 μm columns, analytical 4.6 × 250 mm, 70:30 v/v CH_3CN/0.1 M ammonium formate, 2 mL/min, $t_R = 3.5$ min) to determine the radiochemical purity (>97%) and the specific radioactivity at the time of synthesis. The total synthesis time was 35 min from EOB, with an average radiochemical yield of 18 ± 4% ($n = 4$) and a specific radioactivity of 326 ± 123 GBq/μmol (nondecay corrected from end of $^{11}CH_3I$ synthesis).

7-[^{11}C]Methyl-2-*exo*-[3′-(6-fluoropyridin-3-yl))-5′-pyridinyl]-7-azabicyclo[2.2.1]heptane ([^{11}C]-24d). Precursor (+)-**23d** (1 mg) was dissolved in 200 μL of anhydrous DMF, capped in a small V-vial, and cooled to −40 °C. [^{11}C]Methyl iodide was swept by argon flow into the vial. After the radioactivity reached a plateau, the vial was assayed in the dose calibrator and then heated at 80 °C for 5 min. Water (200 μL) was added and the solution was injected onto the semipreparative HPLC column (Phenomenex Luna C-18 10 μm column, semipreparative 10 × 250 mm, 33:67:0.1 v/v/v CH_3CN/0.1 M ammonium formate/TEA, 14 mL/min). The retention time of the normethyl precursor was 3.6 min. The product peak, having a retention time of 7.54 min, was collected in 50 mL of HPLC water. The water solution was transferred through a Waters C-8 Sep-Pak Plus. The product was eluted with 1 mL ethanol into a vial and diluted with 9 mL of 0.9% saline. The final product [^{11}C]-**24d** was then analyzed by analytical HPLC (Phenomenex Luna C-18 10 μm columns, analytical 4.6 × 250 mm, 20:80 v/v CH_3CN/0.1 M ammonium formate, 2 mL/min, $t_R = 5.5$ min) to determine the radiochemical purity (>97%) and the specific radioactivity at the time of synthesis. The total synthesis time was 32 min from EOB, with an average radiochemical yield of 8 ± 4% ($n = 4$) and specific radioactivity of 427 ± 279 GBq/μmol (nondecay corrected from end of $^{11}CH_3I$ synthesis).

(−)-7-Methyl-2-*exo*-[3′-(6-[^{18}F]fluoropyridin-3-yl))-5′-pyridinyl]-7-azabicyclo[2.2.1]heptane ([^{18}F](−)-24d). A solution of the [^{18}F]fluoride, 20 mg of Kryptofix 222, and 3.5 mg of K_2CO_3 in 1 mL of 50% aqueous acetonitrile was added to a reaction vessel of GE [^{18}F]FDG box. The mixture was heated at 120−135 °C under a stream of argon, while water was evaporated azeotropically after the additions of 2.5 mL of CH_3CN. A solution of the bromo precursor **26** (4 mg) in anhydrous DMSO (0.8 mL) was added to the reaction vessel and heated at 180 °C for 18 min. The reaction mixture was cooled, diluted with 1 mL of water, injected onto the reverse-phase HPLC column (Phenomenex Luna semipreparative C-18 10 μm column, 10 × 250 mm), and eluted with 23:77:0.1 v/v/v CH_3CN/0.1 M ammonium formate /NEt_3 at a flow rate of 12 mL/min. The radioactive peak of [^{18}F]**24d**, with a retention time of 10−11 min, was collected into 50 mL of HPLC water. The water

solution was transferred through a Waters C-18 Sep-Pak Plus. The product was eluted with 1 mL of ethanol into a vial and diluted with 10 mL of 0.9% saline. The final product [^{18}F]**24d**, prepared with an average radiochemical yield 14 ± 4% (n = 7; nondecay-corrected), was then analyzed by analytical HPLC (Phenomenex Luna C-18 10 μm column, analytical 4.6 × 250 mm, 20:80 v/v CH_3CN/0.1 M ammonium formate, 2 mL/min, t_R = 5.6 min) to determine the radiochemical purity (>98%) and the specific radioactivity 510 ± 257 GBq/μmol at the time of synthesis.

In Vitro Binding Assay. The in vitro inhibition binding assays of **16**, **17**, **23d**, and **24a**−**d** (Table 2) were performed commercially by NovaScreen Biosciences, a Caliper Life Science Co., (Hanover, MD) under conditions similar to those previously published.[26] In brief, rat cortical membranes were incubated with [^{3}H]epibatidine (K_d = 63 pM) at a concentration of 0.1 nM in a buffer consisting of 50 mM Tris, 120 mM NaCl, 5 mM KCl, 2 mM $CaCl_2$, 1 mM $MgCl_2$, 0.003 mM atropine sulfate at pH 7.4 for 150 min at 0 °C. The binding was terminated by rapid vacuum filtration of the assay contents onto GF/C filters presoaked in PEI. Radioactivity trapped onto the filters was assessed using liquid scintillation spectrometry. Nonspecific binding was defined as that remaining in the presence of 20 nM (±) epibatidine. The assays were done in duplicate at multiple concentrations of the test compounds. Binding assay results were analyzed using a one-site competition model, and IC_{50} curves were generated based on a sigmoidal dose response with variable slope. The K_i values were calculated using the Cheng−Prusoff equation.[27]

Animal Studies. Mice Studies. Baseline Study. Male, CD-1 mice weighing 25−30 g from Charles River Laboratories (Wilmington, MA) were used for biodistribution studies. The animals were sacrificed by cervical dislocation at various times (three animals per time-point) following injection of [^{11}C](−)-**24d** (~1.5 MBq (~40 μCi), specific radioactivity was about 259 GBq/μmol (7000 mCi/μmol) in 0.2 mL saline) into a lateral tail vein. The brains were rapidly removed and dissected on ice. The brain regions of interest were weighed and their radioactivity content was determined in an automated γ-counter, with a counting error below 3%. Aliquots of the injectate were prepared as standards and their radioactivity content was counted along with the tissue samples. The percent of injected dose per gram of tissue (%ID/g tissue) was calculated. All experimental protocols were approved by the Animal Care and Use Committee of the Johns Hopkins Medical Institutions.

Saturation of [^{11}C](−)-24d Binding with (−)-24d. In vivo saturation studies were done by i.v. administration of various doses of (−)-**24d** (0.002 μmol/kg, 0.047 μmol/kg, 0.079 μmol/kg, 0.19 μmol/kg, and 2 μmol/kg) in saline (0.1 mL), followed by i.v. injection of the radiotracer (~1.5 MBq (~40 μCi)) 15 min thereafter. Control animals were injected with 0.1 mL of the vehicle solution. Animal behavior was observed for 60 min. Sixty min after administration of the tracer, brain tissues were harvested and their radioactivity content was determined.

Small Animal PET. A male Wistar rat (Charles River) was anesthetized by intraperitoneal administration of a combination of ketamine (72 mg/kg), xylazine (6 mg/kg), and acepromazine (6 mg/kg), positioned on the bed of the GE eXplore Vista small-animal PET scanner (GE Medical Systems, Waukesha, WI), and kept anesthetized with isoflurane (0.5%−1%; approximately 1 L/min). The radiotracer (±)-**17** or (−)-**17** (11.1 MBq or 0.3 mCi of in 0.2 mL of saline) was injected via the tail vein. Following injection, the rat was imaged for 90 min using a 28 dynamic frame protocol (3 × 20 s, 3 × 40 s, 5 × 60 s, 6 × 120 s, 8 × 300 s, 3 × 600 s). PET images were reconstructed using a 2D OSEM algorithm after subtracting the scatter component from the sonogram images. Mean images were created and they were used for drawing regions of interest (ROIs) on the Th and the CB. For each region, the ROI was drawn on two adjacent slices, then the ROIs were applied to the dynamic images to generate time−activity curves.

Baboon PET Experiments. The experimental protocol was approved by the Animal Care and Use Committee of the Johns Hopkins Medical Institutions. Male baboons (*Papio anubis*; 20−26 kg) were studied in baseline control experiments. The animals were fasted for 12 h prior to the PET study. Anesthesia was given initially with intramuscular injection of 20 mL (9 mg/kg) Saffan (Schering-Plough, Middlesex, U.K.). The baboon was intubated and anesthesia was maintained with a constant infusion of Saffan diluted with isotonic saline (1:4) at an average flow rate that corresponded to 7.5 mg/kg/h. Circulatory volume was maintained by infusion of isotonic saline. An arterial catheter was inserted for blood sampling. Physiological vital signs including heart rate, ECG, blood pressure, and oxygen saturation were continuously monitored throughout the study.

The animal was positioned in a high-resolution research tomograph (ECAT HRRT) brain PET scanner (CPS Innovations, Inc., Knoxville, TN). The head of the baboon was fitted with a thermoplastic mask that was then attached to a head holder for reproducible fixation.

A 6 min transmission scan with a 1 mCi Germanium-68 source was initially performed for attenuation correction. Then dynamic PET data were acquired in 3D list mode during a 90 min ([^{11}C]-(−)-**24d** (444 MBq (12 mCi), specific radioactivity = ~444 GBq/μmol (12 000 mCi/μmol) or [^{11}C](+)-**24d** (444 MBq (12 mCi), specific radioactivity = ~296 GBq/μmol (8000 mCi/μmol) or 180 min ([^{18}F](−)-**24d**, specific radioactivity = 518 GBq/μmol (~14 000 mCi/μmol)) period following a bolus injection of the radioligand in a list mode. Arterial blood was sampled rapidly initially and with prolonging intervals throughout the scan.

To analyze the PET images, the SPGR (spoiled gradient) MRI volume was acquired in the same baboon with the Signa 1.5 T scanner (GE Medical Systems, Milwaukee, WI).

Baboon Plasma Metabolite Analysis: Metabolites of [^{11}C]-(−)-**24d** and [^{18}F]-(−)-**24d** in baboon were studied using a general method previously developed for PET radiotracers.[28] Specifically, arterial blood samples were withdrawn at 5, 15, 30, 60, and 90 min intervals up to 90 min postinjection and plasma was analyzed for the presence of the parent radioligands and their radiolabeled metabolites. Briefly, 3 mL of plasma in 8 M urea is passed through a capture column (19 × 4.6 mm Strata-X, Phenomenex, Torrance, CA) at 2 mL/min, followed by 1% acetonitrile in water to wash plasma proteins from the column. The effluent from the capture column, containing only highly polar components, flows through a dual BGO detector (Bioscan, Washington, DC). The solvent is then switched to a mixture of 35% acetonitrile/65% 0.1M aqueous ammonium bicarbonate (2 mL/min) for elution of the radiolabeled components bound to the capture column onto the analytical column (Gemini C18, 4.6 × 250 mm, Phenomenex, Torrance, CA).

Acknowledgment. The authors wish to thank Drs. Martin G. Pomper and Arthur Weissman for helpful discussions, Mr. James Fox for performing small animal PET imaging, Ms. Paige Finley for the rodent experiments, and Ms. Elena Y. Barskiy for editorial assistance. This research was supported by Department of Radiology of the Johns Hopkins School of Medicine.

Supporting Information Available: Combustion analysis, compound purity, and chiral HPLC data. This material is available free of charge via the Internet at http://pubs.acs.org.

References

(1) Maziere, M.; Comar, D.; Marazano, C.; Berger, G. Nicotine-11C: synthesis and distribution kinetics in animals. *Eur. J. Nucl. Med.* **1976**, *1*, 255−8.
(2) Paterson, D.; Nordberg, A. Neuronal nicotinic receptors in the human brain. *Prog. Neurobiol.* **2000**, *61*, 75−111.
(3) Horti, A. G.; Villemagne, V. L. The quest for Eldorado: Development of radioligands for in vivo imaging of nicotinic acetylcholine receptors in human brain. *Curr. Pharm. Des.* **2006**, *12*, 3877−3900.
(4) Zhang, Y.; Pavlova, O. A.; Chefer, S. I.; Hall, A. W.; Kurian, V.; Brown, L. L.; Kimes, A. S.; Mukhin, A. G.; Horti, A. G. 5-Substituted derivatives of 6-halogeno-3-((2-(*S*)-azetidinyl)methoxy)pyridine and 6-halogeno-3-((2-(*S*)-pyrrolidinyl)methoxy)pyridine with low picomolar affinity for $\alpha4\beta2$ nicotinic acetylcholine receptor and wide range of lipophilicity: Potential probes for imaging with positron emission tomography. *J. Med. Chem.* **2004**, *47*, 2453−2465.

(5) Waterhouse, R. N. Determination of lipophilicity and its use as a predictor of blood−brain barrier penetration of molecular imaging agents. *Mol. Imaging Biol.* **2003**, *5*, 376−389.
(6) Dischino, D. D.; Welch, M. J.; Kilbourn, M. R.; Raichle, M. E. Relationship between lipophilicity and brain extraction of carbon-11-labeled radiopharmaceuticals. *J. Nucl. Med.* **1983**, *24*, 1030.
(7) Laruelle, M.; Slifstein, M.; Huang, Y. Relationships between radiotracer properties and image quality in molecular imaging of the brain with positron emission tomography. *Mol. Imaging Biol.* **2003**, *5*, 363−375.
(8) Pichika, R.; Easwaramoorthy, B.; Collins, D.; Christian, B. T.; Shi, B.; Narayanan, T. K.; Potkin, S. G.; Mukherjee, J. Nicotinic α4*β*2 receptor imaging agents: part II. Synthesis and biological evaluation of 2-[18F]fluoro-3-[2-((*S*)-3-pyrrolinyl)methoxy]pyridine (18F-nifene) in rodents and imaging by PET in nonhuman primate. *Nucl. Med. Biol.* **2006**, *33*, 295−304.
(9) Ding, Y. S.; Kil, K. E.; Lin, K. S.; Ma, W.; Yokota, Y.; Carroll, I. F. A novel nicotinic acetylcholine receptor antagonist radioligand for PET studies. *Bioorg. Med. Chem. Lett.* **2006**, *16*, 1049−1053.
(10) Roger, G.; Saba, W.; Valette, H.; Hinnen, F.; Coulon, C.; Ottaviani, M.; Bottlaender, M.; Dolle, F. Synthesis and radiosynthesis of [(18)F]-FPhEP, a novel α(4)*β*(2)-selective, epibatidine-based antagonist for PET imaging of nicotinic acetylcholine receptors. *Bioorg. Med. Chem.* **2006**, *14*, 3848−3858.
(11) Kozikowski, A. P.; Chellappan, S. K.; Henderson, D.; Fulton, R.; Giboureau, N.; Xiao, Y.; Wei, Z. L.; Guilloteau, D.; Emond, P.; Dolle, F.; Kellar, K. J.; Kassiou, M. Acetylenic pyridines for use in PET imaging of nicotinic receptors. *ChemMedChem* **2006**, *2*, 54−57.
(12) Huang, Y.; Zhu, Z.; Xiao, Y.; Laruelle, M. Epibatidine analogues as selective ligands for the α(x)*β*2-containing subtypes of nicotinic acetylcholine receptors. *Bioorg. Med. Chem. Lett.* **2005**, *15*, 4385−4388.
(13) Carroll, F. I.; Ma, W.; Yokota, Y.; Lee, J. R.; Brieaddy, L. E.; Navarro, H. A.; Damaj, M. I.; Martin, B. R. Synthesis, nicotinic acetylcholine receptor binding, and antinociceptive properties of 3′-substituted deschloroepibatidine analogues. Novel nicotinic antagonists. *J. Med. Chem.* **2005**, *48*, 1221−1228.
(14) Carroll, F. I.; Lee, J. R.; Navarro, H. A.; Ma, W.; Brieaddy, L. E.; Abraham, P.; Damaj, M. I.; Martin, B. R. Synthesis, nicotinic acetylcholine receptor binding, and antinociceptive properties of 2-exo-2-(2′,3′-disubstituted 5′-pyridinyl)-7-azabicyclo[2.2.1]heptanes: Epibatidine analogues. *J. Med. Chem.* **2002**, *45*, 4755.
(15) Davis, B. A.; Durden, D. A. Reductive methylation of secondary amines containing reducible, hydrolyzable and sterically hindered groups. *Synth. Commun.* **2000**, *30*, 3353−3362.
(16) Patt, J. T.; Spang, J. E.; Westera, G.; Buck, A.; Schubiger, P. A. Synthesis and in vivo studies of [C-11]*N*-methylepibatidine: Comparison of the stereoisomers. *Nucl. Med. Biol.* **1999**, *26*, 165.
(17) Badio, B.; Shi, D.; Garraffo, H. M.; Daly, J. W. Antinociceptive effects of the alkaloid epibatidine: Further studies on involvement of nicotinic receptors. *Drug Dev. Res.* **1995**, *36*, 59.
(18) Patt, J. T.; Spang, J. E.; Westera, G.; Buck, A.; Schubiger, P. A. Synthesis and in vivo studies of [C-11]N-methylepibatidine: Comparison of the stereoisomers. *Nucl. Med. Biol.* **1999**, *26*, 165−173.
(19) Horti, A.; Ravert, H. T.; London, E. D.; Dannals, R. F. Synthesis of a radiotracer for studying nicotinic acetylcholine receptors: (+-)-exo-2-(2-[18F]Fluoro-5-pyridyl)-7-azabicyclo[2.2.1]heptane. *J. Labelled Compd. Radiopharm.* **1996**, *38*, 355.
(20) Decker, M. W.; Brioni, J. D.; Bannon, A. W.; Arneric, S. P. Diversity of neuronal nicotinic acetylcholine receptors: lessons from behavior and implications for CNS therapeutics. *Life Sci.* **1995**, *56*, 545.
(21) Horti, A. G.; Villemagne, V. L. The quest for Eldorado: Development of radioligands for in vivo imaging of nicotinic acetylcholine receptors in human brain. *Curr. Pharm. Des.* **2006**, *12*, 3877−3900.
(22) Horti, A. G.; Scheffel, U.; Koren, A. O.; Ravert, H. T.; Mathews, W. B.; Musachio, J. L.; Finley, P. A.; London, E. D.; Dannals, R. F. 2-[18F]Fluoro-A-85380, an in vivo tracer for the nicotinic acetylcholine receptors. *Nucl. Med. Biol.* **1998**, *25*, 599.
(23) Scheffel, U.; Horti, A. G.; Koren, A. O.; Ravert, H. T.; Banta, J. P.; Finley, P. A.; London, E. D.; Dannals, R. F. 6-[18F]Fluoro-A-85380: An in vivo tracer for the nicotinic acetylcholine receptor. **2000**, *27*, 51.
(24) Carroll, F. I.; Liang, F.; Navarro, H. A.; Brieaddy, L. E.; Abraham, P.; Damaj, M. I.; Martin, B. R. Synthesis, nicotinic acetylcholine receptor binding, and antinociceptive properties of 2-exo-2-(2′-substituted 5′-pyridinyl)-7-azabicyclo[2.2.1]heptanes. Epibatidine analogues. *J. Med. Chem.* **2001**, *44*, 2229−2237.
(25) Wei, Z. L.; Xiao, Y.; Yuan, H.; Baydyuk, M.; Petukhov, P. A.; Musachio, J. L.; Kellar, K. J.; Kozikowski, A. P. Novel pyridyl ring C5 substituted analogues of epibatidine and 3-(1-methyl-2(*S*)- pyrrolidinylmethoxy)pyridine (A-84543) as highly selective agents for neuronal nicotinic acetylcholine receptors containing *β*2 subunits. *J. Med. Chem.* **2005**, *48*, 1721−1724.
(26) Perry, D. C.; Kellar, K. J. [3*H*]Epibatidine labels nicotinic receptors in rat brain: An autoradiographic study. *J. Pharmacol. Exp. Ther.* **1995**, *275*, 1030.
(27) Cheng, Y.; Prusoff, W. H. Relationship between the inhibition constant (K_1) and the concentration of inhibitor which causes 50 per cent inhibition (I_{50}) of an enzymatic reaction. *Biochem. Pharmacol.* **1973**, *22*, 3099−3108.
(28) Hilton, J.; Yokoi, F.; Dannals, R. F.; Ravert, H. T.; Szabo, Z.; Wong, D. F. Column-switching HPLC for the analysis of plasma in PET imaging studies. *Nucl. Med. Biol.* **2000**, *27*, 627−630.

JM070224T